DOI: 10.26599/FSHW.2025.9250818

Contents lists available at SciOpen

Food Science and Human Wellness

journal homepage: https://www.sciopen.com/journal/2097-0765

China Food Publishing Co.

The antiaging effect of edible bird's nest on the skin of healthy women: a randomized controlled trial

Shoujuan Yu[1]*, Shiwen Zhou[1]*, Juan Chen[1]*, Ting Gao[1], Jingjing He[2], Man Yuan[3], Chengying Zhang[4], Qi Zhang[2], Dekui Jin[4], Liwei Zhang[1], Xiaoxian Lin[3], Dongliang Wang[3#], Yixuan Li[2#], Ran Wang[1#]

[1] *Key Laboratory of Functional Dairy, Co-Constructed by Ministry of Education and Beijing Government, Department of Nutrition and Health, China Agricultural University, Beijing 100193, China.*

[2] *Beijing Advanced Innovation Center for Food Nutrition and Human Health, Beijing 100193, China*

[3] *Hebei Edible Bird's Nest Fresh Stew Technology Innovation Center, Langfang, Hebei 065700, China*

[4] *Department of General Practice, The Third Centers of Chinese PLA General Hospital, Beijing 100039, China*

ABSTRACT: Skin is an important barrier organ of the human body. As we age, the appearance and function of our skin deteriorate, which poses health risks. The use of edible bird's nest (EBN) to nourish the skin is an ancient method in Asia. However, the role and mechanism of EBN products in improving human skin aging are still unclear. Therefore, we conducted a randomized controlled trial that included 92 healthy female volunteers aged 25–45 years. They were randomly divided into the high-dose group, the low-dose group, and the control group, and they completed a 12-week treatment. The results showed that the consumption of high-dose EBN significantly improved skin moisture and elasticity by 22.14% and 5.89%, respectively, and significantly reduced the number of deep wrinkles, light wrinkles and spot area by 18.47%, 0.64%, and 3.05%, respectively. ELISA results showed that EBN decreased the expression of inflammatory factors (IL-6 and TNF-α) and serum factors (NO, MMP-1, MMP-9). Moreover, EBN can reverse the aging-induced decreases in SOD and LOX, thus slowing down the aging process. Fecal metagenome results showed that EBN significantly increased the abundance of beneficial bacteria (*Bacteroides_uniformis* and *Bacteroides_finegoldii*). Serum and fecal non-target metabolomic results showed that EBN significantly increased serum and fecal metabolite (N-methylnicotinamide, 2-deoxyribose 5-phosphate, and dimethylmalonic acid) concentrations compared with the control group. Furthermore, correlation analysis revealed a positive association between N-methylnicotinamide levels and skin elasticity. These findings suggest that EBN may ameliorate skin aging by enhancing the diversity of beneficial gut bacteria and their metabolites.

Keywords: Edible bird's nest, skin aging, gut microbiota, metabolites

1. Introduction

The skin is the largest organ in the body, and it has important physiological functions [1-3]. During aging, unbalanced structural homeostasis leads to wrinkles, dryness, roughness, spots, and sagging [4], as well as

* These authors contributed equally to this work.
#**Corresponding author**
dongliang.wang@xxdun.com (Wang, Dong-Liang);
liyixuan@cau.edu.cn (Li, Yixuan);
wangran@cau.edu.cn (Wang, Ran)

Received 17 February 2025
Received in revised from 15 April 2025
Accepted 9 July 2025

impaired skin function [5,6]. Collagen is the main component of dermis, and it plays an essential role in maintaining skin function [7]. Previous studies have shown that inflammation and oxidative stress can lead to collagen loss [8]. In addition, age-related gut dysbiosis is increasingly recognized as a critical contributor to skin aging. It is typified by a loss of beneficial bacteria (e.g., short-chain fatty acid (SCFA) producing bacteria) alongside an overrepresentation of pro-inflammatory taxa (e.g., *Oscillibacter* and *Alistipes*), and a concomitant depletion of key microbial metabolites (SCFAs). These shifts impair intestinal barrier integrity, permitting endotoxins to translocate into the systemic circulation, where they initiate low-grade chronic inflammation, drive extracellular matrix remodeling and collagen degradation, and ultimately manifest clinically as wrinkles and skin laxity [9-12].

Delaying skin aging has been receiving growing attention. At present, the methods of delaying skin aging mainly include exogenous intervention and endogenous regulation. Exogenous intervention methods, such as medical beauty technologies, have a certain operational safety risk [13]. However, skin care products have low bioavailability and skin permeability, resulting in insufficient antiaging effect [14]. Therefore, endogenous regulation to delay skin aging has become a new trend. Oral substances such as vitamin C, tea polyphenols, and probiotics can reduce collagen loss by lowering oxidative stress and inflammation or by regulating gut microbiota [15-19].

In Asia, consuming edible bird's nest (EBN) is a historical method for beauty and health. EBN is a nest built by swiftlets using their saliva and feathers [20]. It contains nutrients such as proteins, carbohydrates, amino acids, water, fat, and trace minerals [21]. EBN has been proven to have antioxidant, moisturizing, whitening, and antiaging effects, which make it beneficial to skin health. Previous studies have shown that supplementation with EBN extracts can maintain the skin thickness of ovariectomized rats, raise the skin's water content in photo-aging mice, enhance the expression of Superoxide dismutase (SOD) in epidermal cells, and downregulate epidermal cell apoptosis, thereby reducing skin damage. Oral EBN extract (200 mg/kg/day) enhanced skin hydration via a 28% rise in hyaluronic acid synthase and 2-fold upregulation of ceramide synthase, suppressed MMP-1 by 40% through ERK/JNK/AP-1 pathway inhibition, and reduced transepidermal water loss (TEWL) by 20% [22]. Water-extract EBN (100 mg/kg/day) attenuated oxidative-stress-induced MMP-1 expression by 45% via down-regulating ERK/JNK signaling in keratinocytes and increased epidermal collagen I/III content by ~30% [23-26]. Moreover, EBN can regulate the gut microbiome of mice, reducing the proportion of harmful bacteria and increasing the proportion of beneficial bacteria [27,28]. However, there is still a lack of research on the improvement effects of related EBN products on human skin aging, and the EBN gut–skin axis mechanism remains unknown.

Therefore, in this study, we conducted a randomized controlled trial to investigate the ameliorative effects of EBN on skin aging and the underlying mechanisms. The study aimed to provide theoretical support for the improvement of skin aging by EBN and to provide scientific evidence for the development of EBN products.

2. Materials and methods

2.1 Study design

A randomized controlled clinical trial was registered at ClinicalTrials.gov (number: ChiCTR2400080220). The trial was approved by the Human Research Ethics Committee of China Agricultural University (the approval number: CAUHR-20220712). Prior to the formal experiment, all volunteers signed an informed consent form.

2.2 Inclusion and exclusion criteria

The inclusion criteria were as follows: (1) female gender; (2) 25–45 years of age; (3) good condition without allergic reaction; (4) healthy living and dietary habits; (4) no treatment related to skin improvement; (5) not leaving Beijing within 3 months; (6) voluntary participation. The exclusion criteria were as follows: (1) skin allergies; (2) current skin improvement and other related treatments; (3) medical esthetic treatment or any type of skin surgery received within 3 months prior to enrollment; (4) mental illness, immune system disease, cardiovascular disease, malignant tumor, coagulation dysfunction, or other diseases. Specifically, participants were screened to exclude individuals with active dermatological conditions, recent antibiotic use (within the past month), and ongoing probiotic supplementation. In addition, female volunteers were assessed for menstrual and hormonal status, and those with significant hormonal fluctuations or on hormone replacement therapy were excluded to minimize confounding effects. These criteria ensured that our study population was as homogenous as possible regarding potential factors affecting both skin physiology and gut microbiota. All participants were instructed to maintain their habitual diet and physical-activity patterns throughout the study period. Furthermore, during the intervention period, the volunteers were required to refrain from consuming fermented foods such as kimchi, as well as foods that have significant impacts on the intestinal flora, such as probiotics and antibiotics.

2.3 Randomization

Assuming a probability of type-I error α=0.05 and the power β=0.20 (confidence level=0.80), it was calculated that at least 23 women were needed in each group [29-32]. Considering a certain dropout rate during the trial, it was planned to recruit 90 healthy female participants, with 30 participants in each group, to ensure the completion. A computer-generated random number sequence was used to create a simple randomization list. Eligible participants were assigned to treatment groups by a professional statistician following the pre-specified allocation sequence until all participants had been allocated. Participants were randomized in a 1:1:1 ratio to one of three groups: control group, low-dose group, or high-dose group [33].

2.4 Intervention

The EBN was stewed at 95℃ for 38 min according to optimized protocols that align with traditional preparation practices. The high-dose group consumed 100 g of stewed EBN products daily (with the following ingredients: purified water, sugar and 5.0 g of dry EBN). The low-dose group consumed 45 g of EBN products daily (ingredients: purified water, sugar and 2.2 g of dry EBN). The control group maintained their habitual diet without receiving any placebo intervention and refrained from consuming any EBN-related products.

2.5 Measurement of skin phenotype

Before the test, the volunteers were not allowed to use any facial skin care products. First, the volunteers cleaned their faces with water and then sat in a room (constant temperature of 20℃, humidity of 40%–60%) for 30 min. To reduce diurnal variation and minimize operator bias, all skin assessments were conducted at a fixed time of day (between 9:00 and 11:00 AM) by the same trained evaluator. All skin assessments were conducted by assessors who were blinded to the group assignments. The Corneometer® CM 825 (Courage + Khazaka Electronic GmbH, Germany) was used to quantify the moisture content of the skin's epidermal stratum corneum, while the Cutometer® dual MPA 580 (Courage + Khazaka Electronic GmbH, Germany) was employed to assess skin elasticity, by using capacitance measurements at three random points to the left and right of the cheek [34,35]. Transparent cards were used to mark and save the detection points, ensuring that the same subject's detection points were consistent each time. The elasticity measurement index R2 refers to the ratio of the skin's rebound amount without negative pressure to the maximum stretching amount with negative pressure [36]. Skin wrinkles and spots area were detected by VISIA skin detector (Canfield Scientific, USA) for facial photography (using parallel polarized light). Parameters such as the number of light and deep wrinkles and the spot area (total spot area/total face area × 100%) were analyzed using the instrument's supporting software (Vplus) [37], which counts the number of light and deep wrinkles and the proportion of spot area.

2.6 Detection of serum indexes

Blood samples were collected via venipuncture after the participants had fasted overnight. Blood samples were centrifuged at 3000 *g* for 15 min to isolate serum [38]. Spare serum was stored at −80℃. Interleukin (IL)-6, IL-10, tumor necrosis factor-α (TNF-α), super oxide dismutase (SOD), malondialdehyde (MDA), nitric oxide (NO), lysyl oxidase (LOX), matrix metalloproteinase (MMP)-1, and MMP-9 were detected by enzyme-linked immunosorbent assay (ELISA) kits (Beijing Siliang Changyuan Biotechnology Co., Ltd., Beijing, China). According to the manufacturer's instructions. Briefly, standards (6, 4, 2, 1, and 0.5 ng/L) and five-fold–diluted serum samples (50 μL per well) were incubated at 37 ℃ for 30 min. Wells were then washed five times with the supplied buffer before the addition of 50 μL detection reagent. After a further wash, 50 μL of substrate was added and color allowed to develop in the dark at 37 ℃ for 15 min. The reaction was terminated by adding 50 μL stop solution, and absorbance was measured at 450 nm. A standard curve was generated to calculate sample concentrations.

2.7 Fecal metagenome detection

Fresh fecal samples were collected and placed in sterile retention bottles. The samples were immediately placed on ice and homogenized by Bertin Precellys Evolution sample homogenizer (Bertin Technologies SAS, France). The samples were stored at −80℃ before use. Fecal metagenome was measured by Beijing Genomics Institution (Shenzhen, China) [39]. DNA was extracted from the samples. Subsequently, the qualified DNA samples were randomly broken into fragments with a length of about 500 bp using an ultrasonic crusher. The entire library was prepared through steps such as end repair, addition of A at the 3' end,

addition of sequencing adapters, purification, fragment selection, PCR amplification or cyclization of connecting products, and digestion of unpaired linear DNA. After the library construction was completed, library sequencing was performed on an Illumina Hiseq platform (Beijing Genomics Institution, China) using the nearest common ancestor algorithm for gene sequence annotation (implemented by Kraken software). All predicted gene sequences from all samples were clustered using CD-HIT (http://www.bioinformatics.org/cd-hit/) with default settings (95% sequence identity and 90% alignment coverage). The longest sequence in each cluster was chosen as the representative to construct a non-redundant gene catalogue. The non-redundant gene catalog was aligned against the NCBI NR database using DIAMOND (BLASTP, version 2.2.28+; http://blast.ncbi.nlm.nih.gov/Blast.cgi) with an e value cutoff of 1×10^{-5}. Taxonomic annotations were assigned based on the NR database's taxonomy information. For each taxon, its abundance in a given sample was calculated as the sum of the abundances of all genes annotated to that taxon. Relative abundances were then aggregated at each taxonomic rank—Domain, Kingdom, Phylum, Class, Order, Family, Genus, and Species—to generate corresponding abundance profiles for all samples [40-41].

For the analysis of α diversity of gut microbiota (Chao1 index, Shannon index) and relative abundance of various bacterial genera, the R 4.0 software Vegan package was used. For the analysis of β diversity, the Euclidean distance was calculated based on species abundance and was visualized using Principal Coordinates Analysis (PCoA) graphs. Linear discriminant analysis effect size (LEfSe) analysis was used for difference analysis, and linear discriminant analysis (LDA) was used to obtain different species between the groups.

2.8 Detection of non-target metabolome in serum and fecal samples

Serum and fecal metabolite tests were conducted by Shanghai Biotree Biomedical Technology Co., Ltd. (Shanghai, China). Metabolites were detected by ultrahigh-performance liquid chromatography (HPLC). For serum samples, 100 μL of each serum sample was transferred into a centrifuge tube, and 400 μL of extraction solution (methanol: acetonitrile=1:1 (V/V)) was added, which contained an isotope-labeled internal standard. Then, the system was vortexed for 30 s and sonicated for 10 min (in an ice water bath). After that, it was kept at −40℃ for 1 h and centrifuged at 4℃ and 12000 r/min for 15 min. The supernatant was transferred to an injection bottle for testing, and an equal amount of supernatant from all samples was mixed to form a quality-control sample for testing. Chromatographic separation of target compounds was performed using a Vanquish UHPLC system (Thermo Fisher Scientific, USA) equipped with a Waters ACQUITY UPLC BEH Amide column (2.1 mm × 50 mm, 1.7 μm). Mobile phase A consisted of water containing 25 mmol/L ammonium acetate and 25 mmol/L ammonia, and mobile phase B was acetonitrile. The autosampler tray was maintained at 4 ℃, and the injection volume was 2 μL. Mass spectrometric data (MS^1 and MS^2) were acquired on an Orbitrap Exploris 120 mass spectrometer (Thermo Fisher Scientific, USA) controlled by Xcalibur software (version 4.4). Instrument parameters were set as follows: sheath gas flow rate, 50 Arb; auxiliary gas flow rate, 15 Arb; capillary temperature, 320 ℃; MS^1 resolution, 60 000; MS^2 resolution, 15 000; normalized collision energies (NCE), 20/30/40; and spray voltage, 3.8 kV in positive mode or –3.4 kV in negative mode.

After converting the raw data into XML format using ProteoWizard software, they were compared with the BiotreeDB (V3.0) database for metabolite identification (Shanghai, China).

For fecal samples, 25 mg of each sample was weighed at low temperature into a centrifuge tube with homogenization beads. For the analysis of serum and fecal metabolites, PCA was performed using SIMCA software (V16.0.2) [42]. The value criteria used were based on two indicators, namely p value of Student's t test and Variable Importance in the Projection (VIP) of the first principal component of the OPLS-DA model. Typically, $P < 0.05$ and VIP > 1 indicate significant differences in metabolite content [42].

2.9 Statistical analysis

The intention-to-treat (ITT) set was used for the analysis in this study. In the ITT set, missing values were imputed based on the last observation carried forward method. Statistical analysis was conducted using SAS V8. Continuous variables with normal or approximately normal distribution were presented as the mean ± standard deviation. Paired-sample t test and paired-sample rank-sum test were used for the comparison before and after a single group trial. For skin phenotypes and serum biomarkers analyses, we applied the One-way ANOVA with Bonferroni correction to control for multiple comparisons and reduce the risk of false-positive results. We performed the rank-sum test on the data that followed a skewed distribution. $P < 0.05$ indicated statistically significant differences, while $P < 0.01$ indicated extremely significant differences. For microbiota, and metabolomics analyses, we applied the False Discovery Rate (FDR) correction to control for multiple comparisons and reduce the risk of false-positive results. The number of tests subjected to FDR correction corresponded to the number of taxa or metabolites assessed in each analysis, with a threshold of $q < 0.05$.

3. Results

3.1 Baseline characteristics

A total of 432 valid questionnaires were received for this study, of which 284 were excluded for not meeting the enrolment requirements, and 148 women participated in the cheek skin elasticity re-screening (Table 1 & Figure 1). Based on the on-site elasticity results, considering the target of 90-person enrollment, volunteers with elasticity values R2 below 0.600 were included. Finally, 92 women signed an informed consent form to participate in the experiment. They were divided into the following three groups through a minimum random grouping method: the high-dose group (31 individuals), the low-dose group (31 individuals), and the control group (30 individuals). During the trial, eight individuals were removed from the group, with a dropout rate of 8.70%. In the end, 28 individuals in each group completed the trial. As shown in Table 1, there were no significant differences among the three groups in terms of age, body mass index (BMI), skin phenotype, exercise habits, smoking status, or alcohol consumption.

Table 1 Baseline characteristics of the subjects

	High-dose group (28 women)	Low-dose group (28 women)	Control group (28 women)	*P* value
Age (years)	36.5 ± 5.8	36.2 ± 5.9	35.4 ± 5.0	> 0.05

BMI (kg/m2)	22.4 ± 2.9	22.1 ± 3.1	22.9 ± 3.6	> 0.05
Dietary habit (regular/irregular)	24/4	25/3	24/4	> 0.05
Exercise (times/week)	4	4	4	> 0.05
Smokers (non-smoker/ex-smoker/smoker)	28/0/0	28/0/0	28/0/0	> 0.05
Drinking (non-drinker/quit drinking/currentdrinker)	27/0/1	27/0/1	27/0/1	> 0.05
Elasticity R2	0.536 ± 0.04[a]	0.538 ± 0.05[a]	0.536 ± 0.04[a]	> 0.05
Moisture (Au)	52.923±7.39	51.578±8.45	51.188±10.28	> 0.05
deep wrinkles (count)	284.75±139.91	322.536±160.15	297.206±133.13	> 0.05
light wrinkles (count)	662.321±110.36	631.357±100.63	674.321±90.72	> 0.05
spots area (%)	12.220±1.68	11.779±1.65	12.196±1.89	> 0.05
Monthly income (yuan)	>10000 (54.8%) 5000–10000 (35.5%) 3000–5000 (6.5%) <3000 (3.2%)	>10000 (54.8%) 5000–10000 (29.0%) 3000–5000 (12.9%) <3000 (3.2%)	>10000 (56.7%) 5000–10000 (33.3%) 3000–5000 (10.0%) <3000 (0%)	> 0.05
Education level	Doctor (16.1%) Master's (29.0%) Undergraduate (41.9%) College degree or below (16.1%)	Doctor (29.0%) Master's (25.8%) Undergraduate (35.5%) College degree or below (12.9%)	Doctor (3.3%) Master's (23.3%) Undergraduate (60.0%) College degree or below (13.3%)	> 0.05
Duration of solar radiation in the past year (hours/day)	<2 (77.4%) 2–5 (22.6%) >5 (0%)	<2 (74.2%) 2–5 (25.8%) >5 (0%)	<2 (76.7%) 2–5 (23.3%) >5 (0%)	> 0.05

Note: The same letter annotation in the upper right corner of each line indicates no significant difference. BMI: body mass index (weight in kilograms divided by the square of the height in meters)

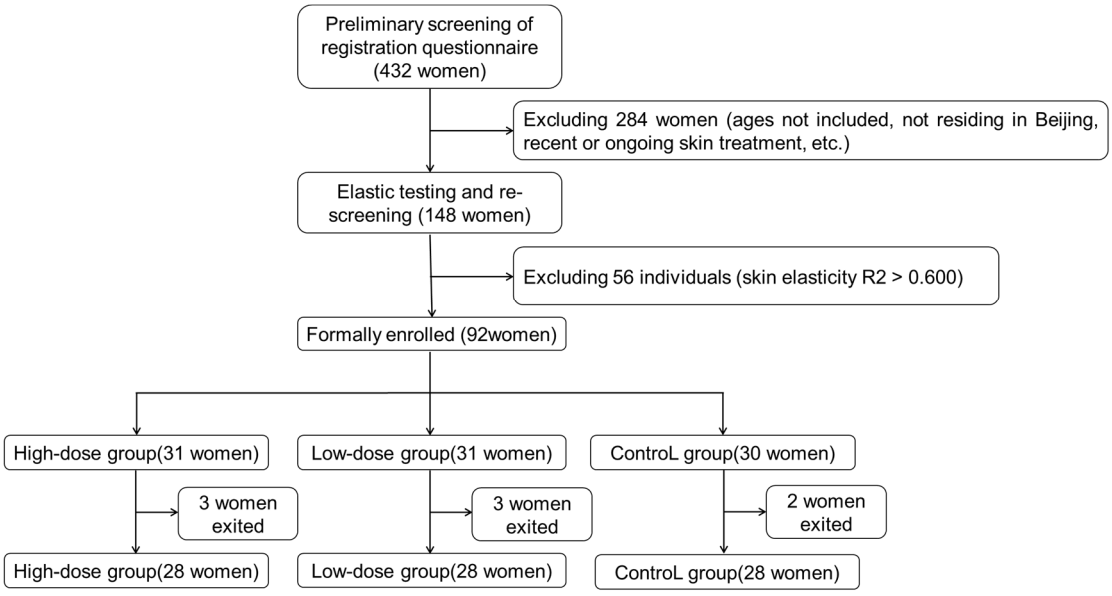

Fig. 1. Flowchart of subject selection.
Note: The elasticity measurement index R2 refers to the ratio of the skin's rebound amount without negative pressure to the maximum stretching amount with negative pressure.

3.2 Effect of EBN on skin function

To evaluate the skin function of the volunteers, Corneometer CM 825, Cutometer MPA 580 and VISIA were used to detect skin indicators (skin moisture, elasticity, wrinkles, and spots area). A high skin moisture content is beneficial for promoting cell metabolism and repair, enhancing the skin's barrier function; elasticity and wrinkles are the most obvious and profound external indicators of skin aging; and aging is also accompanied by increased spots.

As shown in Figure 2A–E, we analyzed the changes of skin phenotypes in the high-dose and low-dose groups after intervention. After 12 weeks of EBN intervention, the skin moisture, elasticity (R2), deep wrinkles, light wrinkles, and spot area of V3-High changed by 22.14% ($P < 0.0001$), 5.89% ($P = 0.0001$), −18.47% ($P = 0.0336$), −0.64% ($P > 0.05$), and −3.05% ($P > 0.05$), respectively, compared with V0-High. The skin moisture, elasticity (R2), deep wrinkles, light wrinkles, and spot area of V3-Low changed by 20.62% ($P < 0.0001$), 4.60% ($P = 0.0130$), −15.93% ($P = 0.0451$), −2.49% ($P > 0.05$), and 0.67% ($P > 0.05$), respectively, compared with V0-Low. We then analyzed the difference between the high-dose and control groups after 12 weeks of intervention. The results showed that compared with V3-Con, the moisture and elasticity of V3-High were significantly increased by 13.42% ($P < 0.05$) and 5.07% ($P < 0.05$), respectively, and the number of deep wrinkles was significantly decreased by 35.56%. Finally, we compared the change values among the high-dose, low-dose, and control groups. There were significant differences in the change values of moisture, elasticity (R2), deep wrinkles, and spot area between the high-dose group and the control group. In contrast, only the change value of deep wrinkles in the low-dose group was significantly different from that in the control group, indicating that EBN in the high-dose group could significantly improve the skin phenotype.

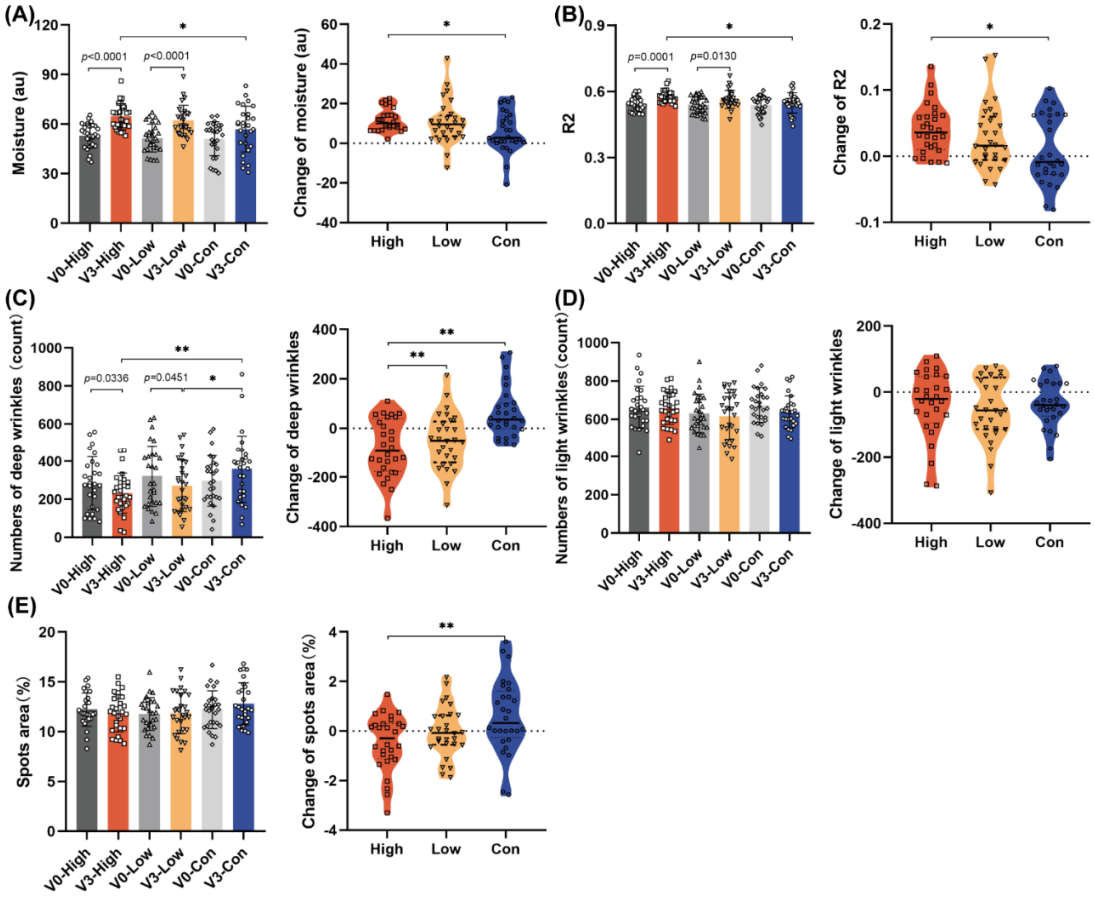

Fig. 2. Effect of EBN on skin phenotype between week 0 (V0) and week 12 (V3). (A–B) Values of cheek moisture and the changes; (B) Values of cheek elasticity R2 and the changes; (C) Numbers of facial deep wrinkles and the changes; (D) Numbers of facial light wrinkles and the changes; (E) Proportions of facial spot area and the changes.

Note: Paired t-tests were used to assess within-group differences before and after the intervention, while one-way ANOVA was employed to evaluate between-group differences following the intervention. "*" indicates a significant difference ($P < 0.05$), "**" indicates a highly significant difference ($P < 0.01$). The error bars represent the standard deviation of the mean (SD).

3.3 Effect of EBN on serum inflammatory factors

Inflammatory response is one of the main causes of collagen loss, which leads to skin aging. Therefore, to evaluate the level of inflammation in the volunteers, the concentrations of IL-6, TNF-α, and IL-10 in serum were tested by ELISA kits. As shown in Figure 3A–C, compared with V0-High, the levels of IL-6 and TNF-α in V3-High significantly decreased by 22.51% ($P < 0.0001$) and 23.79% ($P < 0.0001$), respectively, and there was no significant change in the level of IL-10 in V3-High. Compared with V0-Low, the levels of IL-6, TNF-α, and IL-10 in V3-Low significantly decreased by 34.20% ($P < 0.0001$), 23.61% ($P < 0.0001$), and 37.19% ($P < 0.0001$), respectively.

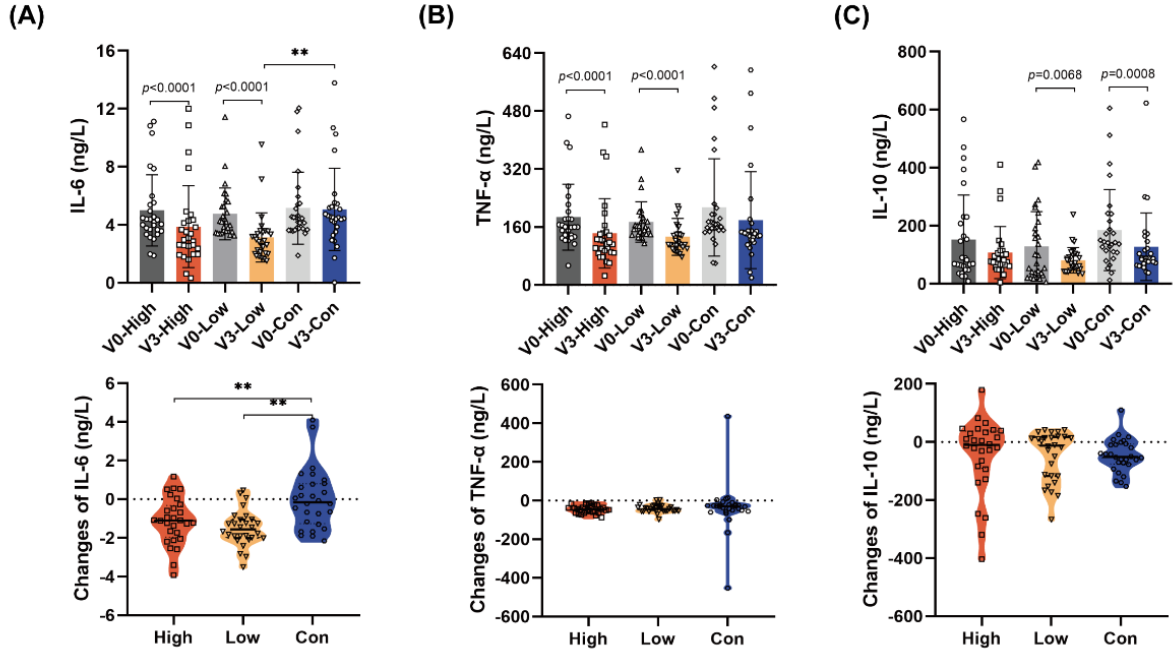

Fig. 3. Effect of EBN on concentrations and the changes of inflammatory factors in serum between week 0 (V0) and week 12 (V3). (A) Values of concentrations of IL-6 and the changes; (B) Values of concentrations of TNF-α and the changes; (C) Values of concentrations of IL-10 and the changes.

Note: Paired t-tests were used to assess within-group differences before and after the intervention, while one-way ANOVA was employed to evaluate between-group differences following the intervention. "**" indicates a highly significant difference ($P < 0.01$). The error bars represent the standard deviation of the mean (SD).

We then compared the change values of inflammatory cytokines among the high-dose, low-dose, and control groups. We found that the IL-6 change values in the high- and low-dose groups were significantly lower than those in the control group (IL-6_changes [con vs. high]: −0.08 vs. −1.12 ng/L, $P < 0.01$; IL-6_changes [con vs. low]: −0.08 vs. −1.63 ng/L, $P < 0.01$]. There were no significant differences in TNF-α and IL-10 changes among the three groups. These findings indicate that consuming EBN may reduce the levels of proinflammatory factors IL-6 and TNF-α, maintain stable levels of anti-inflammatory factor IL-10, and facilitate the reduction of inflammatory response.

3.4 Effect of EBN on serum indicators of oxidative stress

Oxidative stress is one of the main causes of collagen loss, which leads to skin aging. Therefore, to evaluate the level of oxidative stress in the volunteers, the concentrations of NO, MDA, and SOD in serum were tested by ELISA kits. As shown in Figure 4A–C, intra-group comparisons revealed that the

concentrations of NO, MDA, and SOD concentration of V3-High changed by −14.18% (P = 0.0384), 0.18% (P > 0.05), and 3.05% (P > 0.05), respectively, compared with V0-High. The concentrations of NO, MDA, and SOD of V3-Low changed by −2.71% (P > 0.05), −5.19% (P > 0.05), and −18.69% (P = 0.0124), respectively, compared with V0-Low. Inter-group comparisons showed that the NO content of V3-High and V3-Low was significantly decreased compared with that of V3-Con, while MDA and SOD concentrations were not significantly different.

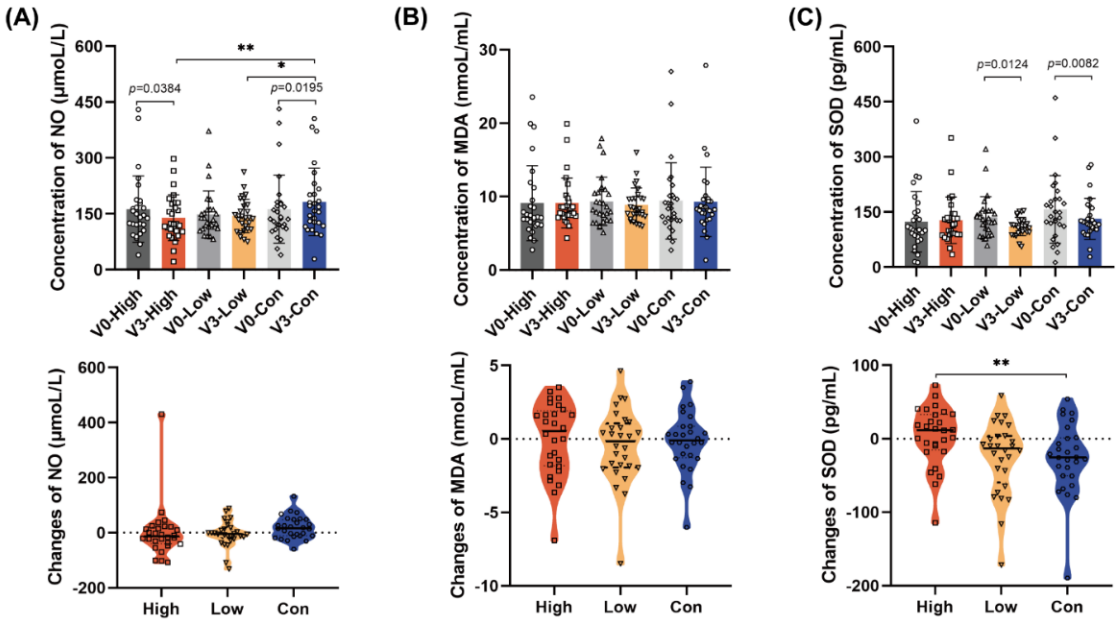

Fig. 4. Effect of EBN on concentrations and the changes of oxidative stress factors in serum between week 0 (V0) and week 12 (V3). (A) Values of concentrations of NO and the changes; (B) Values of concentrations of MDA and the changes; (C) Values of concentrations of SOD and the changes.

Note: Paired t-tests were used to assess within-group differences before and after the intervention, while one-way ANOVA was employed to evaluate between-group differences following the intervention. "*" indicates a significant difference (P < 0.05), "**" indicates a significant difference (P < 0.01). The error bars represent the standard deviation of the mean (SD).

In addition, the change value in the high-dose group was significantly higher than that in the control group (SOD_changes [con vs. high]: −26.18 vs. 3.77 pg/mL, P < 0.05) (Figure 4C). These findings indicate that consuming EBN may increase SOD content, reduce NO content, improve the body's antioxidant capacity, eliminate free radicals, and reduce oxidative stress.

3.5 Effect of EBN on collagen-related factors

To evaluate collagen conditions, the levels of MMP-1, MMP-9, and LOX were detected in serum. As shown in Figure 5A–C, intra-group comparisons revealed that the concentrations of MMP-1, MMP-9, and LOX of V3-Con changed by 8.76% (P > 0.05), 9.64% (P > 0.05), and −7.76% (P > 0.05), respectively, compared with those of V0-Con. However, the concentrations of MMP-1, MMP-9, and LOX of V3-High changed by 6.04% (P > 0.05), −4.66% (P > 0.05), and −2.01% (P > 0.05), respectively, compared with those of V0-High. The concentrations of MMP-1, MMP-9, and LOX of V3-Low changed by 10.03% (P > 0.05), −0.02% (P > 0.05), and −9.40% (P > 0.05), respectively, compared with those of V0-Low.

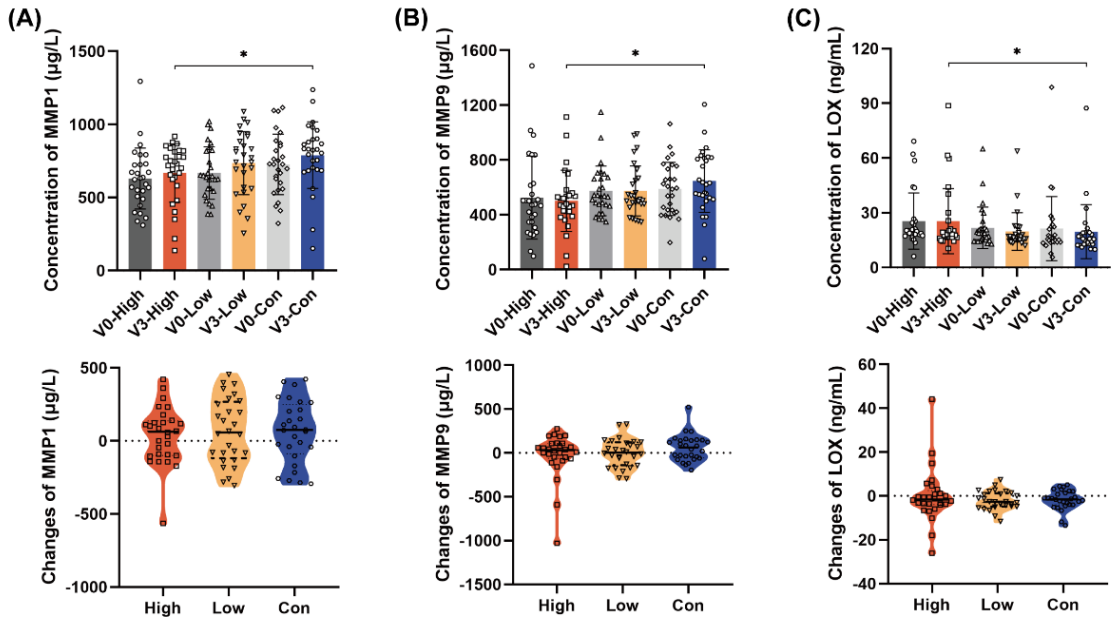

Fig. 5. Effect of EBN on concentrations and the changes of collagen-related factors in serum between week 0 (V0) and week 12 (V3). (A) Values of concentrations of MMP-1 and the changes; (B) Values of concentrations of MMP-9 and the changes; (C) Values of concentrations of LOX and the changes.
Note: Paired t-tests were used to assess within-group differences before and after the intervention, while one-way ANOVA was employed to evaluate between-group differences following the intervention. "*" indicates a significant difference (P < 0.05). The error bars represent the standard deviation of the mean (SD).

Inter-group comparisons showed that there was no significant difference between V0-High and V0-Con.The concentrations of MMP-1 and MMP-9 of V3-High were significantly decreased compared with those of V3-Con. LOX concentration of V3-High was significantly increased compared with that of V3-Con. We also found that the MMP-1, MMP-9, and LOX change values in the high- and low-dose groups were not significantly different from those in the control group. These results suggest that with aging, serum concentrations of MMP-1 and MMP-9 increase and LOX concentrations decrease, and that EBN intervention can delay the changes in these indicators, suggesting that bird's nest has the potential to ameliorate aging.

3.6 Effect of EBN on gut microbiota

The α diversity results of gut microbiota was shown in Figure 6A–B. There were no significant changes in Chao1 and Shannon indexes after the intervention. However, compared with V3-Con, the Shannon diversity of V3-High was significantly reduced. The β diversity results of gut microbiota was shown in Figure 6C. The sample points in each group were relatively dense, indicating that there was no significant difference within the group. When comparing β-diversity between the high-dose and control groups, PCoA analysis revealed a statistically significant separation (P = 0.022; Figure S1), indicating a meaningful difference in community composition and thereby reinforcing our conclusion that the two groups exhibit distinct gut microbiota structures.

In terms of composition, the dominant bacteria at the phylum level were Bacteroidota, Bacillota, Pesudomonadota, and Uroviricota (Figure 6D). At the genus level, the dominant bacteria were *Bacteroides*, *Phocaeicola*, *Faecalibacterium*, *Clostridium*, *Ruminococcus*, and *Lachnospira* (Figure 6E). LEfSe analysis revealed significant differences in bacteria (P < 0.05 and LDA score≥3) between V3-High and V3-Con

(Figure 6F–G); that is, compared with V3-Con, V3-High was significantly enriched with *Bacteroides_uniformis* and *Bacteroides_finegoldii*.

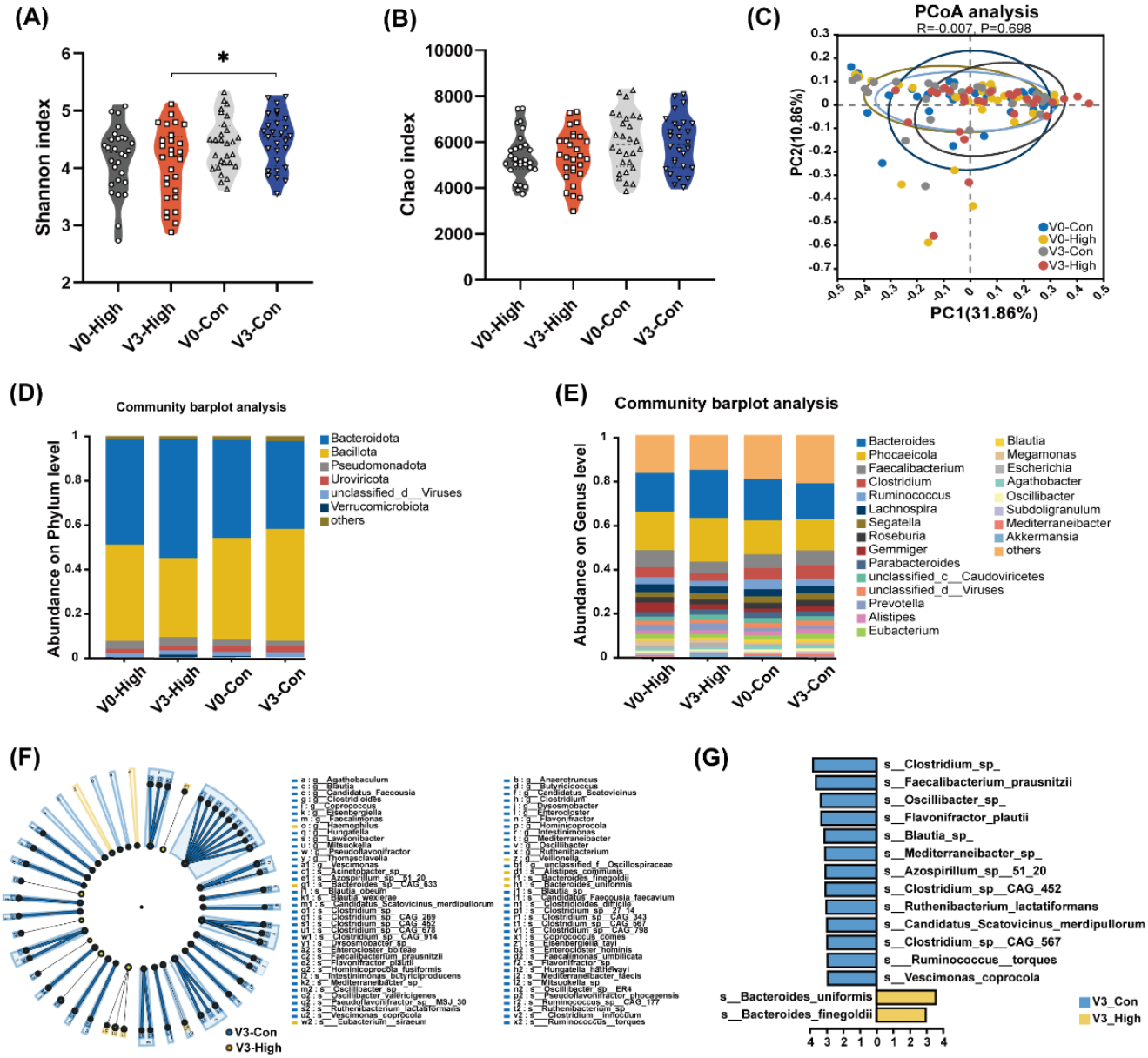

Fig. 6. Effects of EBN on gut microflora. (A–B) α diversity of gut microbiota; (C) β diversity of intestinal microbiota; (D) Composition of microbiota at the phylum level; (E) Composition of microbiota at the genus level; (F–G) LEfSe analysis.

In order to further explore the functions of the microbiota, we employed KEGG (Figure S2A) and CAZy (Figure S2B) analysis to predict microbiota functional pathways, including those involved in SCFA synthesis. As shown in Figure S2A, other glycan degradation, galactose metabolism, glycosaminoglycan degradation are up-regulated in the V3-high group. These pathways provide fermentable sugars and pyruvate precursors that fuel bacterial SCFA synthesis via glycolytic and acetyl-CoA dependent routes. The results shown in Figure S2B indicate glycoside hydrolases was significantly enriched in V3-high group. Systemic SCFAs act on keratinocyte GPR receptors to enhance epidermal differentiation and tight-junction protein expression, improving hydration and elasticity while reducing wrinkle formation. These results support a mechanistic link between gut microbiota-derived metabolites and skin health.

3.7 Effect of EBN on fecal metabolites

A total of 2276 metabolites were detected in fecal using an untargeted metabolomics method. The PCA results of fecal metabolites are shown in Figure 7A–C. The horizontal axis PC [1] and the vertical axis PC [2] represent the scores of the first and second ranked principal components, respectively. The results showed that there was no significant difference between the different groups. Volcano plots in Figure 7D–E show the differences in fecal metabolites between before and after intervention. Compared with V0-High, 361 metabolites increased and 26 metabolites decreased in V3-High (Figure 7D). Compared with V3-Con, 686 metabolites increased and 33 metabolites decreased in V3-High (Figure 7E). Figure 7F shows the heat maps of metabolites in V0-High and V3-High. Specifically, EBN intervention significantly upregulated the levels of 2-keto-3-deoxygluconic acid, 2-keto-3-deoxygalactonic acid, alanine, sarcosine, and beta-alanine.

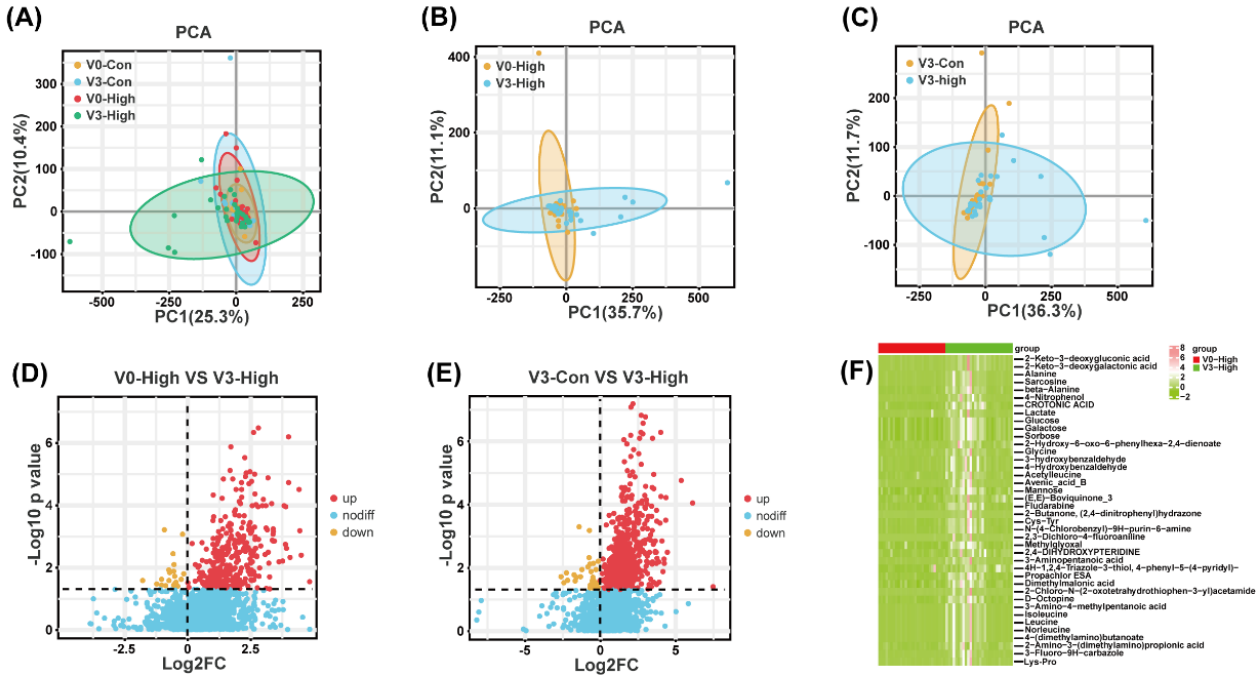

Fig. 7. Fecal metabolites in the high-dose and control groups at week 0 (V0) and week 12 (V3). (A–C) PCA results of fecal metabolites in the high-dose and control groups for different intervention periods; (D–E) Volcano plots of fecal metabolites; (F) Heat maps of different fecal metabolites in V3-High and V0-High.

3.8 Effect of EBN on serum metabolites

The PCA results of serum metabolites are shown in Figure 8A–C. The sample points were mostly within the 95% confidence interval, and the degree of separation between the four groups was not high, indicating that there was no significant difference in serum metabolites between before and after the intervention and between different groups. A total of 1063 metabolites were detected in the serum, of which 59 metabolites were significantly upregulated and 287 metabolites were significantly downregulated in V3-High compared with V0-High (Figure 8D). Compared with V3-Con, 127 metabolites were significantly upregulated and 90 metabolites were significantly downregulated in V3-High (Figure 8E). Heat map in Figure 8F shows the top 40 metabolites that were significantly increased in V3-High, such as N-methylnicotinamide, 2-methylnicotinamide, 6-methylnicotinamide, Ser-Ala, L-leucyl-L-alanine, propyl paraben, Leu-Val, 2-piperidone, Phe-Leu, and others.

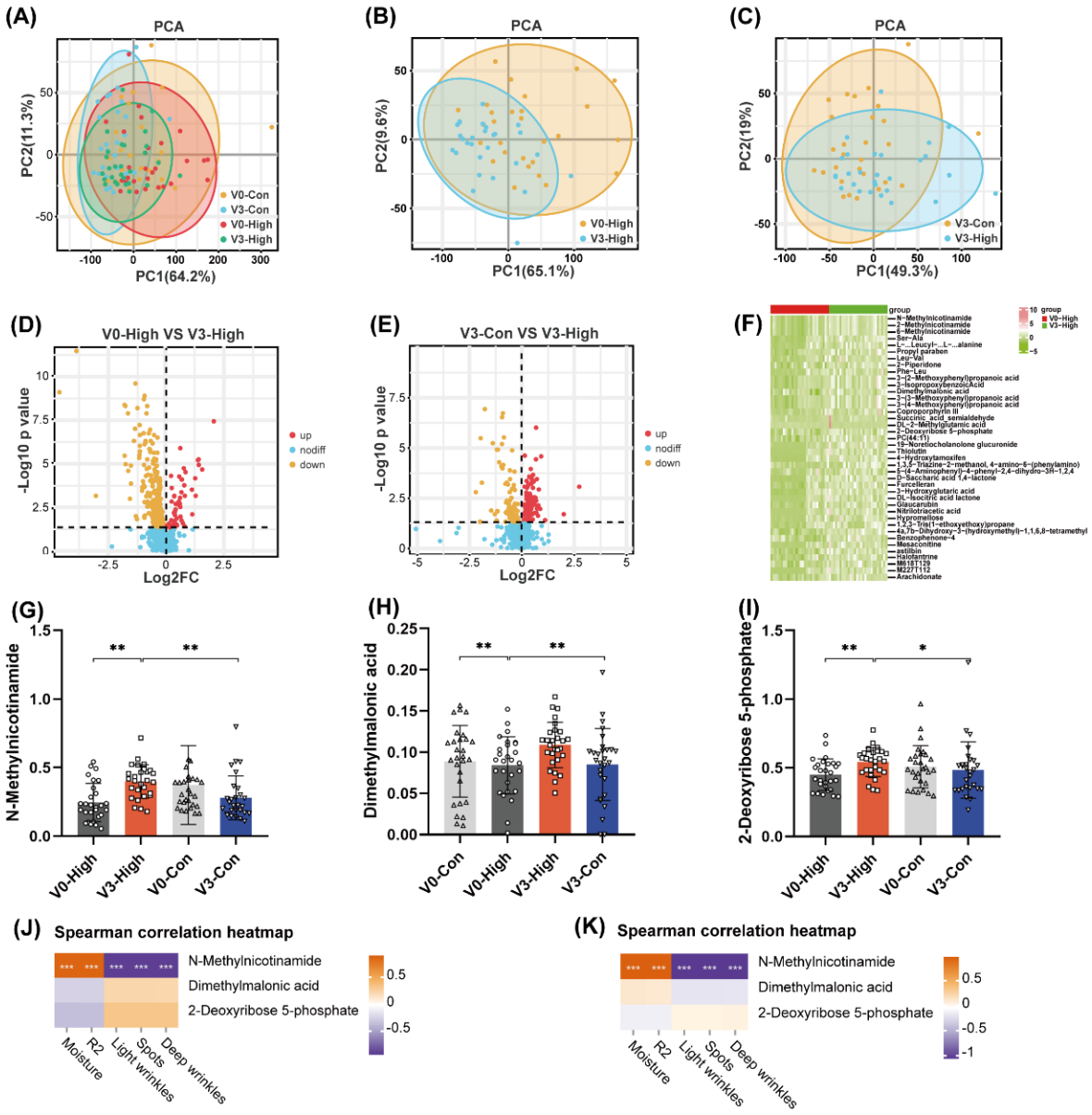

Fig. 8. Serum metabolites in the high-dose and control groups at week 0 (V0) and week 12 (V3). (A–C) PCA results of serum metabolites in the high-dose and control groups for different intervention periods; (D–E) Volcano plots of serum metabolites; (F) Heat maps of different serum metabolites in V3-High and V0-High; (G–I) Relative abundance of N-methylnicotinamide, dimethylmalonic acid, and 2-deoxyribose 5-phosphate in the serum; (J) Correlation analysis of the significantly increased fecal metabolites and the skin phenotypes compared with V0-High and V3-Con; (K) Correlation analysis of the significantly increased serum metabolites and the skin phenotypes compared with V0-High and V3-Con.

Note: "*" indicates $P < 0.05$, "**" indicates $P < 0.01$. High-dose group n=28, control group n=28. The error bars represent the standard deviation of the mean (SD).

To further screen out metabolites significantly enriched in the serum and fecal of V3-High before and after intervention, we compared the significant enrichment of metabolites in serum and fecal between V3-High and V0-High and between V3-High and V3-Con. We found that N-methylnicotinamide, 2-deoxyribose 5-phosphate, and dimethylmalonic acid were simultaneously enriched in the serum and fecal of V3-High, and these substances may be associated with altered skin phenotypes (Figure 8G–I).

Spearman correlation analysis revealed the correlation between the enriched metabolites and the skin phenotype. Figure 8G–H shows the relationship between the skin phenotype and serum and fecal metabolites.

Analysis of fecal metabolites and phenotypic parameters revealed that fecal N-methylnicotinamide was significantly positively correlated with skin moisture (R = 0.89, $P < 0.001$) and elasticity R2 (R = 0.90, $P < 0.001$), and significantly negatively correlated with light wrinkles (R = –0.91, $P < 0.001$), spots area (R = –0.90, $P < 0.001$), and deep wrinkles (R = –0.91, $P < 0.001$). Similarly, analysis of serum metabolites and phenotypic parameters showed that serum N-methylnicotinamide was significantly positively correlated with skin moisture (R = 0.87, $P < 0.001$) and elasticity R2 (R = 0.86, $P < 0.001$), and significantly negatively correlated with light wrinkles (R = –0.90, $P < 0.001$), spots area (R = –0.89, $P < 0.001$), and deep wrinkles (R = –0.88, $P < 0.001$).

Furthermore, we performed Spearman correlation to assess relationships between key bacteria and differential metabolites (Figure. S3). Notably, the relative abundance of *Bacteroides uniformis* correlated strongly with N-methyl-nicotinamide levels in both fecal (R= 0.94, $P < 0.001$) and serum (R= 0.85, $P < 0.001$) samples. These associations reinforce a mechanistic link between gut microbial shifts and metabolite regulation, underscoring their potential role in modulating skin function. Taken together, our results demonstrate that EBN may improve skin phenotypes by modulating the composition and levels of metabolites, attenuating skin-related inflammation and oxidative stress, and downregulating the expression of collagen-related factors.

4. Discussion

The skin is an important barrier organ in the human body. Aging can cause damage to the skin's function and appearance, posing significant health risks. External interventions such as medical beauty treatments and applying skincare products have issues such as unsafe operation and insufficient effect. Thus, internal dietary therapy has become a new trend. It is a time-honored method to consume EBN for nourishing the skin. In recent years, EBN has been proven to delay skin aging. However, there is a lack of confirmation on the improvement effects of EBN products on human skin, and the related mechanisms of improving skin health are still unclear. Therefore, we conducted a randomized controlled trial to investigate the improvement effect of EBN on skin aging and the underlying mechanism.

The results of this study showed that after EBN intervention, the skin function (moisture, wrinkles, elasticity, and deep spots) in the EBN high- and low-dose groups was significantly improved compared with the state before the experiment. This is consistent with the results of two previously reported EBN interventions on population skin moisture test [29,43]. However, the sodium hyaluronate and collagen components added to the EBN beverage in those two studies may have interfered with the effects, whereas the food tested in our study only contained EBN (a new stewing process), purified water, and a small amount of rock sugar. Thus, our study could prove the effectiveness of EBN in improving skin moisture and elasticity. However, owing to lack of matched inert placebo, this study did not include a placebo control. Future trials will incorporate a rigorously formulated placebo to address this issue explicitly. Another study using EBN extract in a capsule form (trial duration of 12 weeks) showed no significant improvement in skin moisture after intervention. Our study indicated that EBN had a positive improvement effect on elasticity and wrinkles,

which is more significant than that in the study of consuming EBN extract in a capsule form (trial duration of 12 weeks) [31], once again confirming the effectiveness of the new stewed EBN supplement form.

Inflammation and oxidative stress can induce skin collagen loss, which leads to skin aging. Proinflammatory factors, chemokines, and other factors promote chronic inflammation in the dermis, affecting the functional status of adjacent cells, leading to fibroblast aging, and accelerating the degradation of collagen I and III [44]. Cell and animal experiments [26] confirmed that EBN digestive fluid significantly reduced the mRNA expression of IL-1β, IL-6, and TNF-α in keratinocytes induced by TNF-α and skin tissues of mice with dermatitis. In this study, the levels of IL-6 and TNF-α were significantly reduced in the high-dose and low-dose EBN groups after the intervention, and IL-6 levels were significantly lower than those in the control group at the end. The IL-10 concentration in the high-dose group did not show significant changes compared with the baseline, while the control group showed a significant decrease. These findings indicate that consuming EBN can reduce the levels of serum proinflammatory factors (IL-6 and TNF-α), maintain stable levels of anti-inflammatory factor (IL-10), and exert anti-inflammatory effects, thereby reducing inflammatory reactions and promoting skin health.

When a large amount of free radicals such as NO are produced in the body and antioxidant enzymes such as SOD are not sufficiently cleared, free radicals are prone to accumulation. The final product MDA causes damage to lipids, proteins, and nucleic acids, leading to cellular aging and activating the MMPs, thereby triggering the downregulation of collagen production and leading to dermal aging. The researchers found that EBN could increase the antioxidant and reduced the oxidative stress levels in non-pregnant rats [45]. Kim [22,46] confirmed that the water extract of EBN could eliminate free radicals in skin HaCaT cells, reduce MMP-1 expression, and achieve antiaging by downregulating the expression of the ERK/JNK/AP-1 pathway. In this study, there was no significant change in SOD content in the high-dose group after the trial. After 12 weeks, the NO content in the high-dose group significantly decreased compared with baseline, while there was no significant change in the low-dose group. The NO content in the high-dose and low-dose groups after the trial was significantly lower than that in the control group. Hence, consuming EBN may increase SOD content, reduce NO content, enhance the body's antioxidant capacity, eliminate free radicals, reduce oxidative stress, and delay the aging of skin.

The net content of collagen is one of the absolute indicators for measuring the youthful state of the skin. During aging, there is a significant loss of skin collagen. The loss can be explained by two pathways, namely reduced generation and increased degradation. The generation pathway of collagen is mainly initiated and regulated by the LOX family of proteins. During aging, the expression of LOX decreases, hindering the activation of transforming growth factor-β and receptors/Smad2/Smad3 pathway and downregulating the expression of procollagen genes [47]. In this study, there was no significant change in LOX content in the high-dose group after the trial compared with baseline, while the control group showed a decreasing trend. The LOX content in the high-dose group after the trial was significantly higher than that in the control group, indicating that consuming EBN can increase serum LOX levels and help maintain collagen production levels.

The degradation pathway of collagen is usually mediated by oxidative stress and inflammatory response, and MMPs are specifically upregulated through the ROS/MAPK/AP-1/NF-κB pathway. MMPs are responsible for degrading extracellular matrix (ECM), especially collagen. Among them, MMP-1 is the main protease that causes collagen fiber fragmentation. Next, the gelatinase MMP-9 (the core of ECM degradation) is responsible for further degradation of the collagen fragments [48-50]. Inhibiting the activity of AP-1 and reducing the expression of MMP-2, MMP-3, and MMP-9 can reduce the generation of wrinkles [51]. For example, Bae JY [52] used tannic acid in photoaging model mice and effectively inhibited wrinkle formation by reducing the expression of MMP-1. In this study, the levels of MMP-1 and MMP-9 in the high-dose group after intervention were significantly lower than those in the control group. These findings indicate that consuming EBN can reduce serum levels of MMP-1 and MMP-9, which is beneficial for delaying collagen degradation. This study also suggests that consuming EBN may increase LOX content during the aging process and reduce MMP content by reducing oxidative stress and inflammatory response, thereby maintaining collagen production, inhibiting collagen degradation, reducing collagen loss.

The perspective of the gut–skin axis indicates an association between gut microbiota and skin health. For example, Ting Gao [10] achieved reverse regulation of the disrupted gut microbiota in aging mice by orally administering Bifidobacterium longum 68S, maintaining microbial homeostasis, improving ceramide synthesis disorders, and repairing skin barrier dysfunction. The analysis of α diversity and β diversity showed that consuming EBN did not alter the overall structure of gut microbiota. In our study, the 12-week trial of stewed EBN (within 5 g of dry EBN) did not affect the diversity, richness, and overall structure of the gut microbiota. Consuming EBN significantly enriched *Bacteroides_uniformis* and *Bacteroides_finegoldii*, which produce short-chain fatty acids [53,54]. *Bacteroides_uniformis* appears to enhance epithelial barrier function and suppress inflammation through SCFA production, TLR2/IL-10 upregulation [55-57]. Although direct skin model validation is pending for *Bacteroides_finegoldii*, its genus-level PSA suggest analogous benefits for skin barrier repair and anti-inflammatory activity [58].

To further detect the changes of metabolites in the faces and serum of the volunteers before and after EBN intervention, non-targeted metabolomics analysis was performed in this study. It was found that N-methylnicotinamide, 2-deoxyribose 5-phosphate, and dimethylmalonic acid were simultaneously enriched in the serum and fecal of V3-High. N-Methylnicotinamide, a principal plasma metabolite of nicotinamide, has been shown to be effective in the treatment of skin disorders such as acne vulgaris and rosacea and possesses notable anti-inflammatory properties [59]. In our experiment, correlation analysis showed that N-methylnicotinamide significantly positively correlated with skin moisture and elasticity. These results indicate that EBN may improve skin function by regulating the gut microbiome and metabolites. However, the precise molecular mechanisms by which N-methylnicotinamide attenuates cutaneous inflammation have yet to be elucidated [60,61].

A growing body of evidence supports multiple indirect “gut–skin axis” mechanisms by which intestinal microbes influence skin physiology. SCFAs produced by gut bacteria enter the bloodstream and modulate

distal barrier tissues. In skin, SCFAs engage GPR on keratinocytes and resident immune cells, inhibiting NF-κB–driven pro-inflammatory cytokine release and promoting tight-junction protein expression, thereby enhancing barrier integrity and reducing dermatitis in animal models [57,62]. In addition, gut microbes modulate systemic T-cell subsets (e.g., increasing Tregs via SCFA mediated histone deacetylase inhibition), leading to a more tolerogenic immune environment that can attenuate skin inflammation. Microbial metabolites can influence hypothalamic-pituitary-adrenal (HPA) axis activity, thereby altering cortisol levels and skin barrier homeostasis under stress [63]. In our study, we found beneficial bacteria associated with short acid production and other metabolites in the intestine, which may be associated with the improvement of skin after consumption of EBN.

5. Conclusion

We conducted a randomized controlled trial to investigate the improvement effect of EBN on skin aging and the underlying mechanism. We found that EBN had antiaging effects on the skin of healthy women. Consumption of high-dose EBN significantly improved skin moisture elasticity and elasticity by 22.14 and 5.89%, respectively, and significantly reduced the number of deep wrinkles, light wrinkles and the proportion of skin spot area by 18.47%, 0.64%, and 3.05%, respectively. EBN improved skin aging by increasing the abundance of beneficial microbiota Bacteroides_uniformis and Bacteroides_finegoldii in the intestine and by increasing the beneficial metabolites such as N-methylnicotinamide. Specifically, we explain that microbial metabolites such as SCFA production bacteria can enhance skin barrier function by promoting moisture retention and modulating local inflammatory responses. In parallel, compounds like N-methylnicotinamideare known to improve skin physiology by reduce inflammation. These mechanistic insights, linked to the gut–skin axis, provide a clearer rationale for how alterations in the gut microbiota may directly influence skin health. However, there are some limitations to this study. For example, this study recruited only female volunteers, did not evaluate the skin microbiome, nor conduct follow-up validation experiments involving microbial or metabolite supplementation. We will address these aspects in future research.

Compliance with ethics requirement

This research was approved by the Human Research Ethics Committee of China Agricultural University (the approval number: CAUHR-20220712). It was registered at ClinicalTrials.gov (number: ChiCTR2400080220). The trial was approved by the Prior to the formal experiment, all volunteers signed an informed consent form.

Declaration of Competing Interest

The authors declare that they have no known competing financial interests or personal relationships that could have appeared to influence the work reported in this paper.

Acknowledgments

We thank LetPub (www.letpub.com.cn) for its linguistic assistance during the preparation of this manuscript.

Funding sources

This work was supported by grants from the National Key Research and Development Program of China (No. 2022YFF1100100).

References

[1] A.S. Tulah, M.A. Birch-Machin, Stressed out mitochondria: the role of mitochondria in ageing and cancer focussing on strategies and opportunities in human skin, Mitochondrion. 13 (2013) 444-453. https://doi.org/10.1016/j.mito.2012.11.007.

[2] S. Jiang, Z.K. Liao, H.Y. Jia, et al., The regional distribution of melanosomes in the epidermis affords a localized intensive photoprotection for basal keratinocyte stem cells, J Dermatol Sci. 103 (2021) 130-134. https://doi.org/10.1016/j.jdermsci.2021.06.010.

[3] E.D. Lephart, Skin aging and oxidative stress: Equol's anti-aging effects via biochemical and molecular mechanisms, Ageing Res Rev. 31 (2016) 36-54. https://doi.org/10.1016/j.arr.2016.08.001.

[4] W. Montagna, K. Carlisle, Structural changes in ageing skin, Br J Dermatol. 122 Suppl 35 (1990) 61-70. https://doi.org/10.1111/j.1365-2133.1990.tb16127.x.

[5] B.A. Gilchrest, M. Yaar, Ageing and photoageing of the skin: observations at the cellular and molecular level, Br J Dermatol. 127 Suppl 41 (1992) 25-30. https://doi.org/10.1111/j.1365-2133.1992.tb16984.x.

[6] C.C. Zouboulis, E. Makrantonaki, G. Nikolakis, When the skin is in the center of interest: An aging issue, Clin Dermatol. 37 (2019) 296-305. https://doi.org/10.1016/j.clindermatol.2019.04.004.

[7] F. Solano, Metabolism and Functions of Amino Acids in the Skin, Adv Exp Med Biol. 1265 (2020) 187-199. https://doi.org/10.1007/978-3-030-45328-2_11.

[8] T. Quan, G.J. Fisher, Role of Age-Associated Alterations of the Dermal Extracellular Matrix Microenvironment in Human Skin Aging: A Mini-Review, Gerontology. 61 (2015) 427-434. https://doi.org/10.1159/000371708.

[9] Thevaranjan, A. Puchta, C. Schulz, et al., Age-Associated Microbial Dysbiosis Promotes Intestinal Permeability, Systemic Inflammation, and Macrophage Dysfunction, Cell Host Microbe. 21 (2017) 455-466.e454. https://doi.org/10.1016/j.chom.2017.03.002.

[10] T. Gao, Y. Li, X. Wang, et al., Bifidobacterium longum 68S mediated gut-skin axis homeostasis improved skin barrier damage in aging mice, Phytomedicine. 120 (2023) 155051. https://doi.org/10.1016/j.phymed.2023.155051.

[11] I. Salem, A. Ramser, N. Isham, et al., The Gut Microbiome as a Major Regulator of the Gut-Skin Axis, Front Microbiol. 9 (2018) 1459. https://doi.org/10.3389/fmicb.2018.01459.

[12] Y. Ratanapokasatit, W. Laisuan, T. Rattananukrom, et al., How Microbiomes Affect Skin Aging: The Updated Evidence and Current Perspectives, Life (Basel). 12 (2022) https://doi.org/10.3390/life12070936

[13] M. Xiong, Q. Zhang, W. Hu, et al., The novel mechanisms and applications of exosomes in dermatology and cutaneous medical aesthetics, Pharmacol Res. 166 (2021) 105490. https://doi.org/10.1016/j.phrs.2021.105490.

[14] P. Rattanawiwatpong, R. Wanitphakdeedecha, A. Bumrungpert, et al., Anti-aging and brightening effects of a topical treatment containing vitamin C, vitamin E, and raspberry leaf cell culture extract: A split-face, randomized controlled trial, J Cosmet Dermatol. 19 (2020) 671-676. https://doi.org/10.1111/jocd.13305.

[15] J.M. Pullar, A.C. Carr, M.C.M. Vissers, The Roles of Vitamin C in Skin Health, Nutrients. 9 (2017) https://doi.org/10.3390/nu9080866.

[16] P.K. Vayalil, A. Mittal, Y. Hara, et al., Green tea polyphenols prevent ultraviolet light-induced oxidative damage and matrix metalloproteinases expression in mouse skin, J Invest Dermatol. 122 (2004) 1480-1487. https://doi.org/10.1111/j.0022-202X.2004.22622.x.

[17] S.H. Nam, J.H. Choi, G.C. Kim, Topical Application of No-Ozone Cold Plasma in Combination with Vitamin C Reduced Skin Redness and Pigmentation of UV-Irradiated Mice, Biomedicines. 11 (2023) https://doi.org/10.3390/biomedicines11061563.

[18] M. Essendoubi, C. Gobinet, R. Reynaud, et al., Human skin penetration of hyaluronic acid of different molecular weights as probed by Raman spectroscopy, Skin Res Technol. 22 (2016) 55-62. https://doi.org/10.1111/srt.12228.

[19] H.Y. Lim, D. Jeong, S.H. Park, et al., Antiwrinkle and Antimelanogenesis Effects of Tyndallized Lactobacillus acidophilus KCCM12625P, Int J Mol Sci. 21 (2020) https://doi.org/10.3390/ijms21051620.

[20] L.S. Chua, S.N. Zukefli, A comprehensive review on edible bird nests and swiftlet farming, J Integr Med. 14 (2016) 415-428. https://doi.org/10.1016/s2095-4964(16)60282-0.

[21] F. Ma, D. Liu, Sketch of the edible bird's nest and its important bioactivities, Food Research International. 48 (2012) 559-567. https://doi.org/10.1016/j.foodres.2012.06.001.

[22] O.K. Kim, D. Kim, M. Lee, et al., Standardized Edible Bird's Nest Extract Prevents UVB Irradiation-Mediated Oxidative Stress and Photoaging in the Skin, Antioxidants (Basel). 10 (2021) https://doi.org/10.3390/antiox10091452.

[23] K.C. Kim, K.A. Kang, C.M. Lim, et al., Water extract of edible bird's nest attenuated the oxidative stress-induced matrix metalloproteinase-1 by regulating the mitogen-activated protein kinase and activator protein-1 pathway in human keratinocytes, Journal of the Korean Society for Applied Biological Chemistry. 55 (2012) 347-354. https://doi.org/10.1007/s13765-012-2030-8.

[24] N. Matsukawa, M. Matsumoto, W. Bukawa, et al., Improvement of bone strength and dermal thickness due to dietary edible bird's nest extract in ovariectomized rats, Biosci Biotechnol Biochem. 75 (2011) 590-592. https://doi.org/10.1271/bbb.100705.

[25] S. Masuda, Y. Makioka-Itaya, T. Ijichi, et al., Edible bird's nest extract downregulates epidermal apoptosis and helps reduce damage by ultraviolet radiation in skin of hairless mice, J Clin Biochem Nutr. 70 (2022) 33-36. https://doi.org/10.3164/jcbn.21-54.

[26] Q.W.S. Lai, Q. Fan, B.Z. Zheng, et al., Edible bird's nest, an Asian health food supplement, possesses anti-inflammatory responses in restoring the symptoms of atopic dermatitis: An analysis of signaling cascades, Front Pharmacol. 13 (2022) 941413. https://doi.org/10.3389/fphar.2022.941413.

[27] C. Li, X. Xu, X. Lin, et al., Edible bird's nest plays an immune regulation by influencing intestinal flora changes in mice, Journal of Functional Foods. 118 (2024) https://doi.org/10.1016/j.jff.2024.106254.

[28] Y. Xie, H. Zeng, Z. Huang, et al., Effect of Maternal Administration of Edible Bird's Nest on the Learning and Memory Abilities of Suckling Offspring in Mice, Neural Plast. 2018 (2018) 7697261. https://doi.org/10.1155/2018/7697261.

[29] L. Stojanovič, N. Majdič, Effectiveness and safety of hyaluronic acid fillers used to enhance overall lip fullness: A systematic review of clinical studies, J Cosmet Dermatol. 18 (2019) 436-443. https://doi.org/10.1111/jocd.12861.

[30] Y. Dai, J. Cao, Y. Wang, et al., A comprehensive review of edible bird's nest, Food Res Int. 140 (2021) 109875. https://doi.org/10.1016/j.foodres.2020.109875.

[31] H.M. Kim, Y.M. Lee, E.H. Kim, et al., Anti-Wrinkle Efficacy of Edible Bird's Nest Extract: A Randomized, Double-Blind, Placebo-Controlled, Comparative Study, Front Pharmacol. 13 (2022) 843469. https://doi.org/10.3389/fphar.2022.843469.

[32] S.Y. Choi, E.J. Ko, Y.H. Lee, et al., Effects of collagen tripeptide supplement on skin properties: a prospective, randomized, controlled study, J Cosmet Laser Ther. 16 (2014) 132-137. https://doi.org/10.3109/14764172.2013.854119.

[33] N.W. Scott, G.C. McPherson, C.R. Ramsay, et al., The method of minimization for allocation to clinical trials. a review, Control Clin Trials. 23 (2002) 662-674. https://doi.org/10.1016/s0197-2456(02)00242-8.

[34] C. Sun, G. Hu, L. Yi, et al., Integrated analysis of facial microbiome and skin physio-optical properties unveils cutotype-dependent aging effects, Microbiome. 12 (2024) 163. https://doi.org/10.1186/s40168-024-01891-0.

[35] X.X. Yang, M.M. Zhao, Y.F. He, et al., Facial Skin Aging Stages in Chinese Females, Front Med (Lausanne). 9 (2022) 870926. https://doi.org/10.3389/fmed.2022.870926.

[36] H.S. Ryu, Y.H. Joo, S.O. Kim, et al., Influence of age and regional differences on skin elasticity as measured by the Cutometer, Skin Res Technol. 14 (2008) 354-358. https://doi.org/10.1111/j.1600-0846.2008.00302.x.

[37] M.-Y. Yang, Q.-L. Shen, D.-T. Xu, et al., Striped WriNet: Automatic wrinkle segmentation based on striped attention module, Biomedical Signal Processing and Control. 90 (2024) https://doi.org/10.1016/j.bspc.2023.105817

[38] S. Yu, J. Wang, Y. Li, et al., Structural Studies of Water-Insoluble β-Glucan from Oat Bran and Its Effect on Improving Lipid Metabolism in Mice Fed High-Fat Diet, Nutrients. 13 (2021) https://doi.org/10.3390/nu13093254.

[39] S. Yu, X. Wang, Z. Li, et al., Solobacterium moorei promotes the progression of adenomatous polyps by causing inflammation and disrupting the intestinal barrier, J Transl Med. 22 (2024) 169. https://doi.org/10.1186/s12967-024-04977-3.

[40] T. Liang, T. Jiang, Z. Liang, et al., Gut microbiota-driven BCAA biosynthesis via Staphylococcus aureus -expressed acetolactate synthase impairs glycemic control in type 2 diabetes in South China, Microbiol Res. 296 (2025) 128145. https://doi.org/10.1016/j.micres.2025.128145.

[41] Y. Lin, H.C. Lau, C. Liu, et al., Multi-cohort analysis reveals colorectal cancer tumor location-associated fecal microbiota and their clinical impact, Cell Host Microbe. 33 (2025) 589-601.e583. https://doi.org/10.1016/j.chom.2025.03.012.

[42] S. Wiklund, E. Johansson, L. Sjöström, et al., Visualization of GC/TOF-MS-based metabolomics data for identification of biochemically interesting compounds using OPLS class models, Anal Chem. 80 (2008) 115-122. https://doi.org/10.1021/ac0713510.

[43] J. Li, S. Guan, J. Su, et al., The Development of Hyaluronic Acids Used for Skin Tissue Regeneration, Curr Drug Deliv. 18 (2021) 836-846. https://doi.org/10.2174/1567201817666201202094513.

[44] J. Zhang, H. Yu, M.Q. Man, et al., Aging in the dermis: Fibroblast senescence and its significance, Aging Cell. 23 (2024) e14054. https://doi.org/10.1111/acel.14054.

[45] A.A. Albishtue, N. Yimer, M.Z.A. Zakaria, et al., Edible bird's nest impact on rats' uterine histomorphology, expressions of genes of growth factors and proliferating cell nuclear antigen, and oxidative stress level, Vet World. 11 (2018) 71-79. https://doi.org/10.14202/vetworld.2018.71-79.

[46] M. Ismail, A. Alsalahi, M.A. Aljaberi, et al., Efficacy of Edible Bird's Nest on Cognitive Functions in Experimental Animal Models: A Systematic Review, Nutrients. 13 (2021) https://doi.org/10.3390/nu13031028.

[47] T. Quan, T. He, S. Kang, et al., Solar ultraviolet irradiation reduces collagen in photoaged human skin by blocking transforming growth factor-beta type II receptor/Smad signaling, Am J Pathol. 165 (2004) 741-751. https://doi.org/10.1016/s0002-9440(10)63337-8.

[48] G.J. Fisher, S.C. Datta, H.S. Talwar, et al., Molecular basis of sun-induced premature skin ageing and retinoid antagonism, Nature. 379 (1996) 335-339. https://doi.org/10.1038/379335a0.

[49] J.W. Shin, S.H. Kwon, J.Y. Choi, et al., Molecular Mechanisms of Dermal Aging and Antiaging Approaches, Int J Mol Sci. 20 (2019) https://doi.org/10.3390/ijms20092126.

[50] L. Wang, W. Lee, Y.R. Cui, et al., Protective effect of green tea catechin against urban fine dust particle-induced skin aging by regulation of NF-κB, AP-1, and MAPKs signaling pathways, Environ Pollut. 252 (2019) 1318-1324. https://doi.org/10.1016/j.envpol.2019.06.029.

[51] J.E. Park, H.B. Pyun, S.W. Woo, et al., The protective effect of Kaempferia parviflora extract on UVB-induced skin photoaging in hairless mice, Photodermatol Photoimmunol Photomed. 30 (2014) 237-245. https://doi.org/10.1111/phpp.12097.

[52] J.Y. Bae, J.S. Choi, S.W. Kang, et al., Dietary compound ellagic acid alleviates skin wrinkle and inflammation induced by UV-B irradiation, Exp Dermatol. 19 (2010) e182-190. https://doi.org/10.1111/j.1600-0625.2009.01044.x.

[53] M. Sakamoto, Y. Tanaka, Y. Benno, et al., Butyricimonas faecihominis sp. nov. and Butyricimonas paravirosa sp. nov., isolated from human faeces, and emended description of the genus Butyricimonas, Int J Syst Evol Microbiol. 64 (2014) 2992-2997. https://doi.org/10.1099/ijs.0.065318-0.

[54] H. Zafar, M.H. Saier, Jr., Gut Bacteroides species in health and disease, Gut Microbes. 13 (2021) 1-20. https://doi.org/10.1080/19490976.2020.1848158.

[55] H. Morita, C. Kano, C. Ishii, et al., Bacteroides uniformis and its preferred substrate, α-cyclodextrin, enhance endurance exercise performance in mice and human males, Sci Adv. 9 (2023) eadd2120. https://doi.org/10.1126/sciadv.add2120.

[56] S. Zhang, Q. Nie, Y. Sun, et al., Bacteroides uniformis degrades β-glucan to promote Lactobacillus johnsonii improving indole-3-lactic acid levels in alleviating colitis, Microbiome. 12 (2024) 177. https://doi.org/10.1186/s40168-024-01896-9.

[57] X. Xiao, X. Hu, J. Yao, et al., The role of short-chain fatty acids in inflammatory skin diseases, Front Microbiol. 13 (2022) 1083432. https://doi.org/10.3389/fmicb.2022.1083432

[58] A. Schwarz, R. Philippsen, T. Schwarz, Induction of Regulatory T Cells and Correction of Cytokine Disbalance by Short-Chain Fatty Acids: Implications for Psoriasis Therapy, J Invest Dermatol. 141 (2021) 95-104.e102. https://doi.org/10.1016/j.jid.2020.04.031.

[59] L. Pietrzak, A. Mogielnicki, W. Buczko, Nicotinamide and its metabolite N-methylnicotinamide increase skin vascular permeability in rats, Clin Exp Dermhttps. 34 (2009) 380-384. https://doi.org/10.1111/j.1365-2230.2008.02922.x.

[60] H. Nadeeshani, J. Li, T. Ying, et al., Nicotinamide mononucleotide (NMN) as an anti-aging health product - Promises and safety concerns, J Adv Res. 37 (2022) 267-278. https://doi.org/10.1016/j.jare.2021.08.003.

[61] J. Gebicki, A. Sysa-Jedrzejowska, J. Adamus, et al., 1-Methylnicotinamide: a potent anti-inflammatory agent of vitamin origin, Pol J Pharmacol. 55 (2003) 109-112. https://doi.org/110.1111/j.1365-2230.2005.01908.x.

[62] A. Trompette, J. Pernot, O. Perdijk, et al., Gut-derived short-chain fatty acids modulate skin barrier integrity by promoting keratinocyte metabolism and differentiation, Mucosal Immunol. 15 (2022) 908-926. https://doi.org/10.1038/s41385-022-00524-9.

[63] B. De Pessemier, L. Grine, M. Debaere, et al., Gut-Skin Axis: Current Knowledge of the Interrelationship between Microbial Dysbiosis and Skin Conditions, Microorganisms. 9 (2021) https://doi.org/10.3390/microorganisms9020353.